

## Photometric study of five open star clusters



Sneh Lata<sup>a,\*</sup>, A.K. Pandey<sup>a</sup>, Saurabh Sharma<sup>a</sup>, Charles Bonatto<sup>b</sup>, Ram Kesh Yadav<sup>a</sup>

<sup>a</sup> Aryabhata Research Institute of Observational Sciences, Manora Peak, Nainital 263002, Uttarakhand, India

<sup>b</sup> Universidade Federal do Rio Grande do Sul, Departamento de Astronomia CP 15051, Porto Alegre 91501-970, RS, Brazil

### HIGHLIGHTS

- The paper presents *UBVRI* CCD photometry of five open clusters.
- The fundamental parameters like reddening, distance and age have been derived.
- The spatial structure, mass function and mass segregation have also been studied.

### ARTICLE INFO

#### Article history:

Received 16 May 2013

Received in revised form 12 June 2013

Accepted 13 June 2013

Available online 25 June 2013

Communicated by P.S. Conti

#### Keywords:

Open clusters: colour magnitude diagram

Mass function

Mass segregation

### ABSTRACT

*UBVRI* photometry of the five open clusters Czernik 4, Berkeley 7, NGC 2236, NGC 7226 and King 12 has been carried out using ARIES 104 cm telescope, Nainital. Fundamental cluster parameters such as foreground reddening  $E(B - V)$ , distance, and age have been derived by means of the observed two colour and colour-magnitude diagrams, coupled to comparisons with theoretical models.  $E(B - V)$  values range from 0.55 to 0.74 mag, while ages derived for these clusters range from  $\sim 10$  to  $\sim 500$  Myr. We have also studied the spatial structure, mass function and mass segregation effects. The present study shows that evaporation of low mass stars from the halo of the clusters increases as they evolve.

© 2013 Elsevier B.V. All rights reserved.

### 1. Introduction

Open clusters (OCs) are excellent tools to understand star formation and evolution because their stars emerge from the same molecular cloud and have a mass spectrum that can be used to study the initial mass function (IMF). Poorly populated OCs do not survive longer than a few hundred Myr, whereas rich ones may survive longer (e.g. Pandey and Mahra, 1986; Theuns, 1992; Tanikawa and Fukushige, 2005; Carraro et al., 2005; Bonatto et al., 2012). OCs are also one of the best tools to probe the age and abundance structure of the Galactic disk. As clusters evolve through dynamical effects (internally and by interactions with the Galactic tidal field), a significant fraction of the cluster stars is gradually lost to the field. Mass segregation and evaporation of low-mass members are the main effects of dynamical interactions (de la Fuente Marcos, 2001; Andersen and Nordström, 2000; Patat and Carraro, 1995; Carraro, 2006). Hence, to understand cluster evolution it is necessary to study the dense central region (the core) as well as the expanded and sparse region (the halo or corona) (Pandey et al., 1988; Maciejewski, 2009). In addition, study of the structure of OCs also gives

the opportunity to understand how external environments and internal stellar encounters affect OCs. The morphological structure, or shape, of the young OCs can be governed by initial conditions in the molecular clouds and by internal gravitational interactions and external tidal perturbations as the cluster evolves (Chen et al., 2004; Sharma et al., 2006, 2008). Based on N-body simulations, de la Fuente Marcos, 1997 finds that the total disruption time for a cluster also depends on its richness. The studies of dynamical properties of the OCs are difficult in the absence of kinematical data. However, some information about the dynamical evolution of open clusters can be drawn from statistical analysis of the spatial distribution of the probable cluster members and their mass function (Kang and Ann, 2002; Ann and Lee, 2002).

In order to continue our efforts to study the dynamical evolution of OCs using the photometric properties, we carried out photometric observations of OCs Czernik 4 (Cz 4), Berkeley 7 (Be 7), NGC 2236, NGC 7226 and King 12, which cover a wide range in age and are relatively poorly studied. The basic parameters of these clusters available in the literature are listed in Table 1. Additionally, since these clusters are of intermediate to old age, they may present observable consequences of mass segregation.

The paper is organised as follows. We describe observations and data reduction technique in Section 2. Section 3 deals with spatial

\* Corresponding author. Tel.: +91 9411323891; fax: +91 5942233439.

E-mail address: [sneh@aries.res.in](mailto:sneh@aries.res.in) (S. Lata).

**Table 1**  
Basic parameters of the target clusters taken from the WEBDA.

Cluster	RA (2000) (hh:mm:ss)	Dec (2000) (°:':")	l (°)	b (°)
Cz 4	01 35 24	+61 16 00	128.179	−0.945
Be 7	01 54 12	+62 22 00	130.138	0.376
NGC 2236	06 29 39	+06 49 48	204.370	−1.699
NGC 7226	22 10 26	+55 23 54	101.405	−0.596
King 12	23 53 00	+61 58 00	116.124	−0.130

structure of the cluster. Section 4 describes basic parameters of clusters using the two colour diagram and colour-magnitude diagram obtained in the present study. We study luminosity and mass function in Section 5. In Section 6 we put our effort in describing dynamical evolution of clusters by means of their MF and structural parameters. Finally, we summarise our results in Section 7.

## 2. Observations and data reduction

The *UBVRI* CCD observations of open clusters Cz 4, Be 7, NGC 2236, NGC 7226 and King 12 were carried out using the 104 cm ARIES Telescope. A 2k × 2k CCD was used as a detector. The field of view is  $\sim 13' \times 13'$  and the plate scale is  $\sim 0.76''/\text{pixel}$  in  $2 \times 2$  pixel binning mode. The log of the observations is given in Table 2. The observed *V*-band images of the clusters are shown in Fig. 1. The typical seeing (estimated from the FWHM of the point spread function; PSF) of the images was found to be  $1.5''\text{--}2''$ . Bias and twilight flats were also taken along with the target field. The preprocessing of the CCD images was performed by using the IRAF<sup>1</sup>, which includes bias subtraction, flat field correction and removal of cosmic rays. The instrumental magnitude of the stars were obtained using the DAOPHOT package provided by Stetson (1987, 1992). Both aperture and PSF photometry were carried out to get the magnitudes of the stars. The PSF photometry yields better results for crowded regions. The standardization of the cluster fields was carried out by observing the standard field SA 98 (Landolt, 1992). Instrumental magnitudes were converted to standard magnitudes using the following transformation equations

$$v = V + q_1 + p_1(V - I) + k_v X$$

$$b = B + q_2 + p_2(B - V) + k_b X$$

$$i = I + q_3 + p_3(V - I) + k_i X$$

$$r = R + q_4 + p_4(V - R) + k_r X$$

$$u = U + q_5 + p_5(U - B) + k_u X$$

In the above equations *u*, *b*, *v*, *r* and *i*, obtained after time and aperture corrections are the instrumental magnitudes while *U*, *B*, *V*, *R* and *I* are the standard magnitudes;  $p_1$ ,  $p_2$ ,  $p_3$ ,  $p_4$  and  $p_5$  are the colour coefficients;  $q_1$ ,  $q_2$ ,  $q_3$ ,  $q_4$  and  $q_5$  are the zero point constants;  $k_v$ ,  $k_b$ ,  $k_u$ ,  $k_r$  and  $k_i$  are the extinction coefficients in *V*, *B*, *U*, *R* and *I* filters, respectively, and *X* is the airmass. The values of the coefficients for each observing night are listed in Table 3. The typical DAOPHOT errors at brighter level ( $V \approx 16$  mag) are  $\leq 0.01$  mag, whereas for fainter end ( $V \approx 20$  mag) the errors become larger ( $\approx 0.05$  mag). The entire *UBVRI* CCD photometric data for the cluster under present study is available in electronic form at the WEBDA open cluster data base website at <http://obswww.unige.ch/webda/>. It can also be obtained from the authors.

<sup>1</sup> IRAF is distributed by the National Optical Astronomy Observatory, which is operated by the Association of Universities for Research in Astronomy (AURA) under cooperative agreement with the National Science Foundation.

**Table 2**  
Log of CCD observations.

Region	Filters and Exposure time × no. of frame (in seconds)	Date
Cz 4	U 1200 × 2; B 900 × 3; V 500 × 3; R 200 × 3; I 200 × 3	24 Dec 2008
	U 300 × 3; B 150 × 3; V 30 × 3; R 30 × 5; I 30 × 4	08 Dec 2007
	U 300 × 7; B 100 × 7; V 60 × 7; R 60 × 7; I 60 × 7	08 Dec 2007
Be 7	U 300 × 3; B 180 × 3; V 120 × 3; R 60 × 3; I 60 × 3	23 Jan 2006
SA 98	U 300 × 5; B 180 × 5; V 120 × 5; R 60 × 5; I 60 × 5	23 Jan 2006
NGC 2236	U 1500 × 2; B 900 × 3; V 500 × 3; R 300 × 3; I 300 × 3	05 Dec 2007
	U 300 × 2; B 120 × 2; V 90 × 2; R 60 × 2; I 60 × 2	20 Feb 2009
SA 98	U 300 × 2; B 150 × 2; V 90 × 2; R 60 × 2; I 60 × 2	20 Feb 2009
NGC 7226	U 1200 × 2; B 600 × 2; V 500 × 4; R 200 × 3; I 200 × 3	11 Nov 2007
	U 300 × 2; B 100 × 2; V 90 × 3; R 50 × 3; I 40 × 3	11 Nov 2007
	U 300 × 9; B 180 × 9; V 120 × 9; R 60 × 9; I 60 × 9	11 Nov 2007
King 12	U 300 × 2; B 180 × 3; V 120 × 3; R 60 × 3; I 60 × 3	04 Nov 2005
SA 98	U 300 × 10; B 120 × 10; V 60 × 10; R 30 × 10; I 30 × 10	04 Nov 2005

### 2.1. Comparison with previous photometry

Barring the cluster Cz 4 all the other clusters have already been studied partially either photoelectrically or photographically. A comparison of the present photometries for clusters Be 7, NGC 2236, NGC 7226 and King 12 with the photometries available in the literature has been carried out. In Fig. 2 we plot  $\Delta V$ ,  $\Delta(U - B)$  and  $\Delta(B - V)$  (in the sense, present data minus literature data) for the common stars as a function of *V* magnitude.

#### 2.1.1. Be 7

Phelps and Janes (1994) carried out CCD photometry of Be 7 in the area of  $11.68 \times 11.68$  arcmin<sup>2</sup> for the first time and reported 722 stars down to  $V \sim 21$  mag. The comparison shows that the present *V* magnitude and (*B* − *V*) colour are in fair agreement with those obtained by Phelps and Janes (1994), whereas in the case of (*U* − *B*) colours there seems to be a some trend in  $\Delta(U - B)$ .

#### 2.1.2. NGC 2236

The photographic observations for NGC 2236 were first carried out by Babu; 26 stars (1991) and Orekhova and Shashkina; 434 stars (1987). Babu (1991) also presented *UBV* photoelectric data for the region containing the cluster NGC 2236. Comparison has been made between the present data and those available in the literature. In Fig. 2 open circles and triangles represent present data minus photographic data given by Babu (1991) and Orekhova and Shashkina (1987) respectively, whereas filled circles represent present data minus photoelectric data given by Babu (1991). There seems to be a large scatter in the  $\Delta V$ ,  $\Delta(B - V)$ ,  $\Delta(U - B)$  without any trend. However, the *V* magnitude and (*B* − *V*) colour made photoelectrically (see Fig. 2 filled circles) by Babu (1991) seem to match with those obtained in present study.

#### 2.1.3. NGC 7226

The CCD photometric observations in an area of  $7.9 \times 7.9$  arcmin<sup>2</sup> were presented by Viskum et al. (1997). They reported photometry for 499 stars down to  $V \sim 18$  mag. The present *V* magnitudes and (*B* − *V*) colours are in fair agreement with those obtained by Viskum et al. (1997).

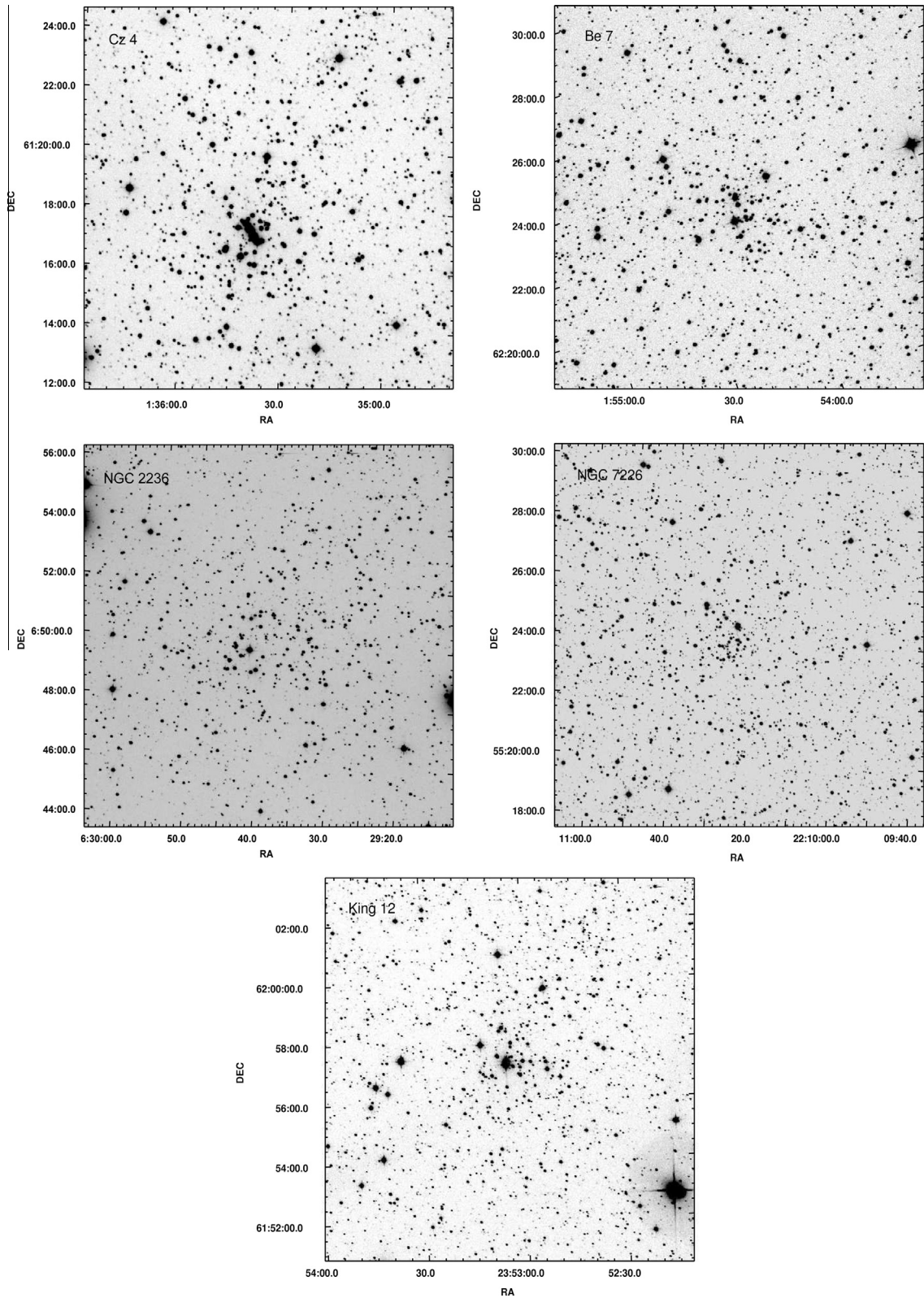


**Fig. 1.** The observed images (V-band) of  $\sim 13 \times 13$  arcmin<sup>2</sup> for the clusters Cz 4, Be 7, NGC 2236, NGC 7226 and King 12. RA and DEC refer to epoch J2000.

#### 2.1.4. King 12

Mohan and Pandey (1984) presented *UBV* photoelectric photometry for 30 stars in the cluster. The present magnitudes and colours match well with those reported by Mohan and Pandey (1984).

#### 2.2. Completeness of the data

It is not possible to detect all the stars present in the CCD frame, especially towards the faint tail. The main reason for the non detection of stars could be e.g, faintness and crowding in the re-

**Table 3**  
The zero point constants, colour coefficients and extinction coefficients on different nights.

Parameters	Date				
	04 Nov 2005	23 Jan 2006	11 Nov 2007	08 Dec 2007	20 Feb 2009
<i>Zero point constant</i>					
$q_1$	$4.17 \pm 0.01$	$4.01 \pm 0.01$	$4.06 \pm 0.01$	$4.62 \pm 0.01$	$5.01 \pm 0.01$
$q_2$	$4.61 \pm 0.01$	$4.45 \pm 0.01$	$5.05 \pm 0.01$	$5.07 \pm 0.02$	$5.70 \pm 0.02$
$q_3$	$4.60 \pm 0.01$	$4.47 \pm 0.01$	$4.97 \pm 0.01$	$5.19 \pm 0.02$	$5.36 \pm 0.01$
$q_4$	$4.07 \pm 0.01$	$3.94 \pm 0.01$	$4.50 \pm 0.01$	$4.52 \pm 0.01$	$5.16 \pm 0.01$
$q_5$	$6.79 \pm 0.01$	$6.62 \pm 0.01$	$7.27 \pm 0.01$	$7.18 \pm 0.02$	$7.69 \pm 0.01$
<i>Colour coefficient</i>					
$p_1$	$-0.04 \pm 0.01$	$-0.02 \pm 0.01$	$-0.02 \pm 0.01$	$-0.02 \pm 0.01$	$-0.05 \pm 0.01$
$p_2$	$-0.04 \pm 0.01$	$-0.03 \pm 0.01$	$-0.02 \pm 0.01$	$-0.02 \pm 0.02$	$-0.02 \pm 0.02$
$p_3$	$-0.05 \pm 0.01$	$-0.05 \pm 0.01$	$-0.05 \pm 0.01$	$-0.05 \pm 0.02$	$-0.05 \pm 0.02$
$p_4$	$-0.04 \pm 0.01$	$-0.01 \pm 0.01$	$-0.02 \pm 0.01$	$-0.03 \pm 0.02$	$-0.07 \pm 0.02$
$p_5$	$0.01 \pm 0.01$	$0.05 \pm 0.01$	$-0.02 \pm 0.01$	$0.01 \pm 0.02$	$-0.04 \pm 0.02$
<i>Extinction coefficients</i>					
$k_u$	$0.65 \pm 0.01$	$0.59 \pm 0.01$	$0.57 \pm 0.02$	$0.58 \pm 0.01$	$0.52 \pm 0.05$
$k_b$	$0.39 \pm 0.01$	$0.33 \pm 0.01$	$0.32 \pm 0.01$	$0.36 \pm 0.01$	$0.35 \pm 0.02$
$k_v$	$0.25 \pm 0.01$	$0.23 \pm 0.01$	$0.19 \pm 0.01$	$0.25 \pm 0.01$	$0.26 \pm 0.02$
$k_r$	$0.19 \pm 0.01$	$0.16 \pm 0.01$	$0.13 \pm 0.01$	$0.15 \pm 0.01$	$0.15 \pm 0.01$
$k_i$	$0.13 \pm 0.01$	$0.10 \pm 0.01$	$0.08 \pm 0.01$	$0.10 \pm 0.01$	$0.11 \pm 0.01$

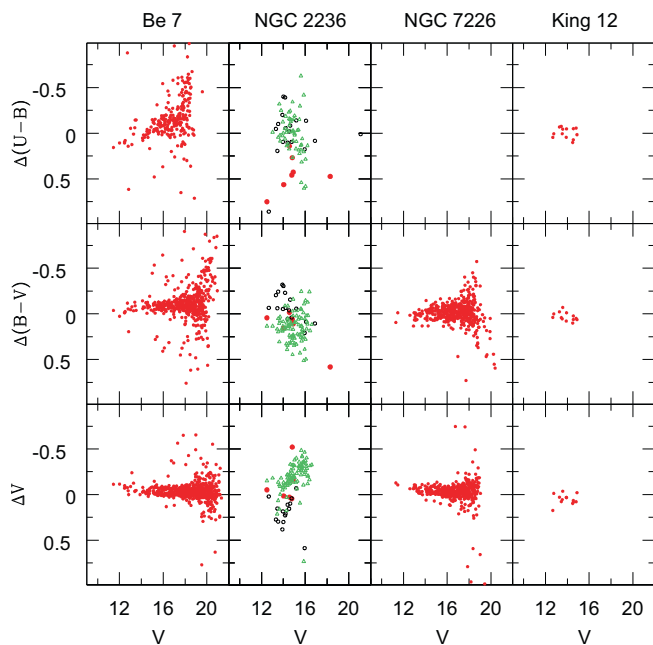


**Fig. 2.** Comparison of the present photometries and photometries available in the literature. The  $\Delta$  represents present data minus data from the literature. In the case of NGC 2236 filled and open circles represent comparison with photoelectric and photographic data (Babu, 1991) respectively while triangles represent comparison with data by Orekhova and Shashkina (1987).

gion. The ADDSTAR routine given in the DAOPHOT software package (Stetson, 1987) was used to correct the data for incompleteness. The artificial stars were added at random positions in the CCD images. The luminosity distribution of artificial stars was chosen in such a way that more stars are inserted towards the fainter magnitude bins. In all, about 10–15% of the total stars were added so that the crowding characteristics of the original frame do not change significantly. The ratio of the stars recovered to those added in each magnitude interval gives the completeness factor (CF) as a function of magnitude. The frames were re-reduced in a similar procedure as used in the case of the original frames. In practice, we followed the procedure given by Sagar and Richtler, 1991. We added artificial stars to both  $V$  and  $I$  images in such a way that they

have similar geometrical locations but differ in  $I$  brightness according to mean  $(V - I)$  colours of the MS stars. The minimum value of the CF of the pair thus obtained is used to correct the data for incompleteness (Sagar and Richtler, 1991). As expected, the incompleteness increases towards fainter magnitudes. The data are found to be complete by 90% up to the magnitude of  $V \sim 19$  mag.

### 3. Spatial Structure of the clusters: radial density profile

The radial density profile has been used to probe the structure and estimate the extent ( $r$ ) of the clusters. Most of the stars are found to be located in the central region, and the stellar density decreases with radial distance which finally merges with the field. The point of maximum stellar density is considered as the cluster centre. To determine the radial density profile, we made several concentric rings around the cluster centre. The stellar density is determined by counting stars inside each concentric annuli and then dividing the number of stars by the area of the respective annulus. We plot the stellar density as a function of radial distance in Fig. 3. The point at which the stellar density merges with the field star density is considered the cluster extent. The field star density is estimated from the region well outside the cluster extent. The estimated radii are: 3.5 arcmin for Cz 4, 4.1 arcmin for Be 7, 4.4 arcmin for NGC 2236, 3.7 arcmin for NGC 7226 and 4.0 arcmin for King 12.

The observed radial density profile of each cluster was fitted by the King profile using the relation  $\rho(r) = f_0 / (1 + (r/r_c)^2)$  (Kaluzny and Udalski, 1992) where  $\rho(r)$  is the projected radial density. The  $r_c$  is the clusters's core radius which is defined as the radial distance at which the value of  $\rho(r)$  becomes half of the central density  $f_0$ . Fig. 3 shows the best fit radial density profile obtained through a  $\chi^2$  minimisation technique. The cluster core radius thus found for the clusters Cz 4, Be 7, NGC 2236, NGC 7226 and King 12 are  $1.09 \pm 0.16$ ,  $0.54 \pm 0.07$ ,  $1.29 \pm 0.15$ ,  $0.72 \pm 0.08$  and  $1.09 \pm 0.10$  arcmin, respectively.

### 4. Fundamental parameters of the clusters

The  $V/B - V$ ,  $V/V - R$  and  $V/V - I$  colour magnitude diagrams (CMDs) for the clusters are shown in Fig. 4, which show a well defined main-sequence (MS), however the contamination due to field stars increases with increase in the magnitude. Therefore, to estimate the field star contamination we have used a region outside

the cluster region. The area of the field region was kept equal to the area of the cluster region. The contribution of field stars from the CMDs of the cluster region was statistically removed using the procedure described by Sandhu et al. (2003) and Pandey et al. (2007). Briefly, for a star in the  $V/V - I$  CMD of the field region, the nearest star within  $V \pm 0.25$  and  $(V - I) \pm 0.125$  in the cluster's  $V/V - I$  CMD was removed. While removing stars from the cluster CMD, the number of stars in each magnitude bin was maintained as per the CF. The statistically cleaned two colour diagram (TCD) ( $U - B/B - V$ ) and CMDs ( $V/B - V$ ,  $V/V - I$ , and  $V/V - R$ ) for target clusters are shown in Figs. 5–8 and used to estimate their fundamental parameters.

#### 4.1. Reddening

The reddening  $E(B - V)$  has been determined using the  $U - B/B - V$  TCD of the clusters by comparing the theoretical model of  $Z = 0.02$  by Girardi et al., 2002 with the observations assuming the normal reddening law, i.e.  $E(U - B)/E(B - V) = 0.72$ , in the regions. The  $U - B/B - V$  TCDs for the cluster region are shown in Fig. 5. In case of King 12 we have taken data for three brighter stars from Mohan and Pandey (1984), which could be probable members of the cluster. These stars were saturated in the present observations of King 12. The fundamental parameters like reddening, distance and age for King 12 have been determined after adding data of these stars. The  $U - B)/(B - V)$  TCD yields  $E(B - V) = 0.55, 0.74, 0.56, 0.60$  and  $0.58$  mag towards the clusters Cz 4, Be 7, NGC 2236, NGC 7226 and King 12, respectively. The estimated uncertainty in estimation of the  $E(B - V)$  values is  $\sim 0.05$  mag. The  $E(B - V)$  obtained in the present study are in fair agreement with the values available in the literature (0.80 mag for Be 7, by Phelps and Janes, 1994; 0.37 mag for NGC 2236, by Rahim, 1970 and 0.68–0.84 mag, by Babu, 1991; 0.49 mag and 0.46 mag for NGC 7226, by Yilmaz, 1970 and Viskum et al., 1997; 0.58 mag for King 12, by Mohan and Pandey, 1984). In case of NGC 2236 Babu, 1991 found a variable reddening  $E(B - V)$  across the field of the cluster ranging between 0.68 mag and 0.84 mag. Mohan and Pandey (1984) reported non-uniform reddening in case of King 12.

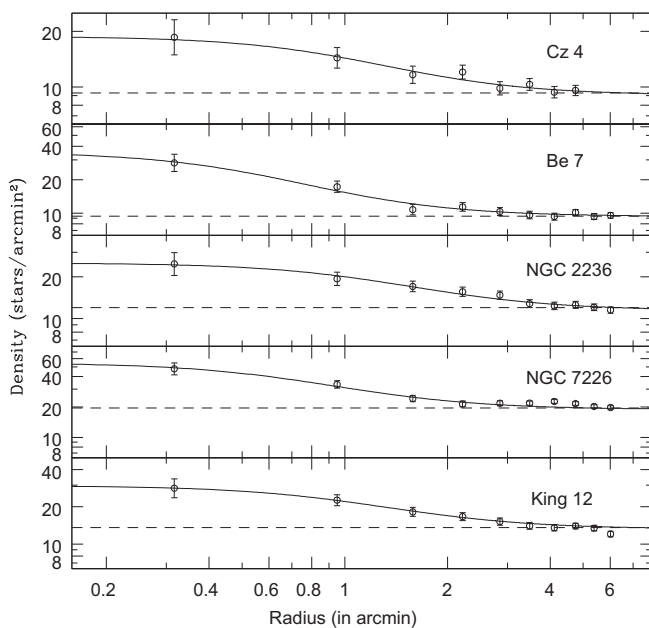


**Fig. 3.** Radial density profile for the present cluster sample. The dashed line and solid in each panel represent the field star density and King profile by Kaluzny and Udalski (1992) respectively.

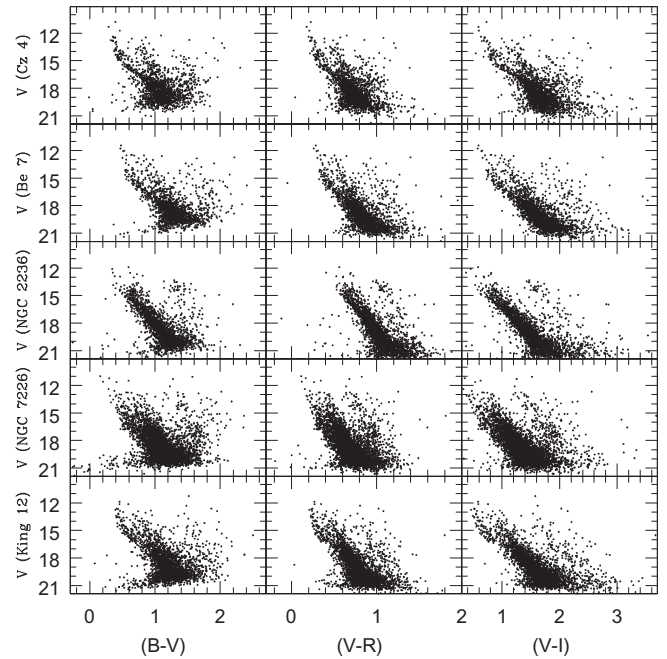


**Fig. 4.** Colour-magnitude diagrams of the present cluster sample showing all stars detected in the frames.

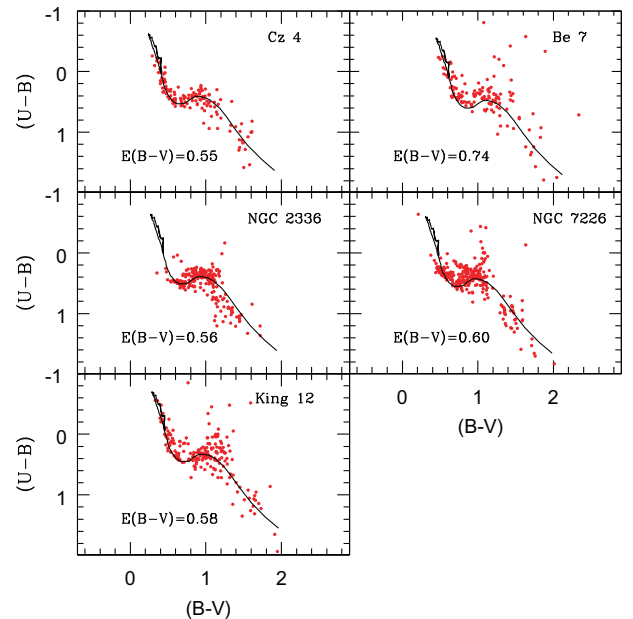


**Fig. 5.**  $U - B$ ,  $B - V$  colour-colour diagram of the present cluster sample. The solid line represents ZAMS by Girardi et al. (2002).

The minimum and maximum reddening values estimated by them are 0.52 mag and 0.69 mag.

#### 4.2. Distance and age

The distances and ages of the clusters have been estimated by visual fitting of the theoretical isochrones of metallicity  $Z = 0.02$  by Girardi et al., 2002 with the MS. The  $V/B - V$ ,  $V/V - R$  and  $V/V - I$  CMDs along with the visually fitted isochrones are shown in Figs. 6–8. The  $E(B - V)$  values for each cluster as mentioned in Section 4.1 has been used in fitting the isochrones. The estimated

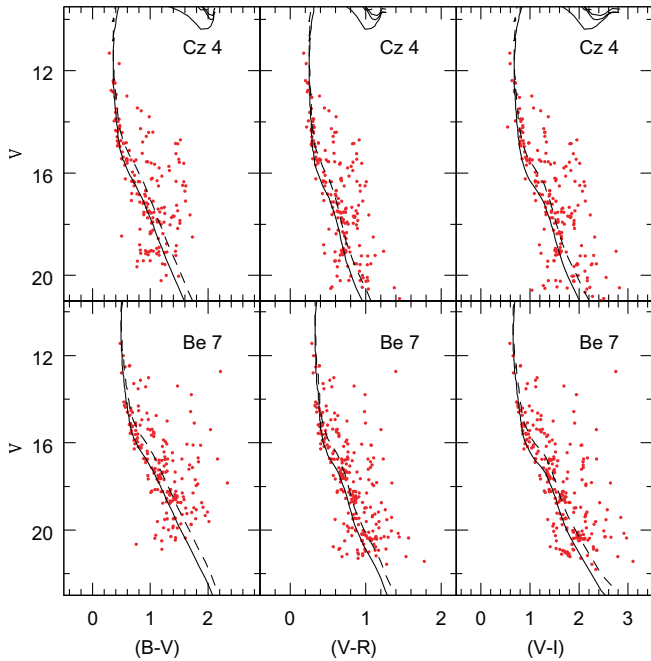


**Fig. 6.** The statically cleaned colour-magnitude diagram for Cz 4 and Be 7. The solid line represents model by Girardi et al. (2002) and dashed line is the same model but for the binary stars.

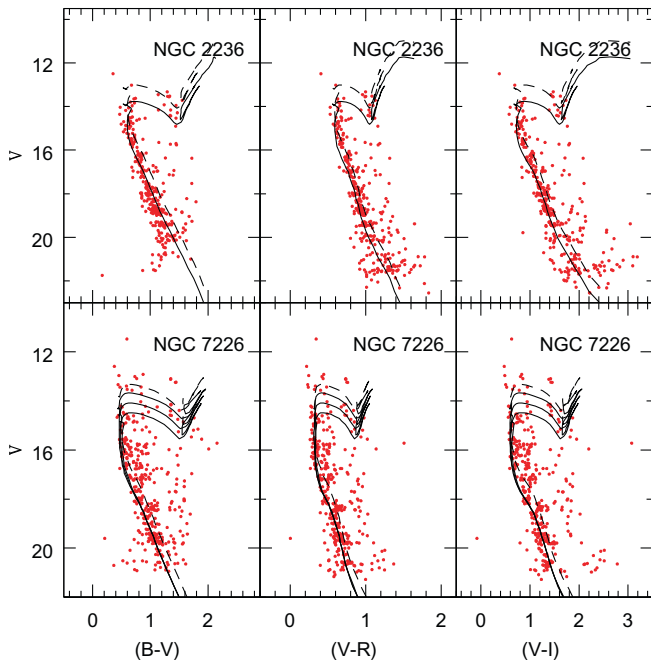


**Fig. 7.** The statically cleaned colour-magnitude diagram for King 12 and NGC 2236 NGC 7226. The solid line represents model by Girardi et al. (2002) and dashed line is the same model but for the binary stars. In case of NGC 7226 the solid line represents model by Girardi et al. (2002) for  $\log(\text{age}) = 8.3, 8.4$  and  $8.5$  and dashed line is the model of  $\log(\text{age}) = 8.4$  by Girardi et al. (2002) but for the binary stars.

values of distance modulus ( $m - M$ ) and  $\log(\text{age})$  for each cluster are given in Table 4. The values for distance and age for each cluster given in the literature are also mentioned in Table 4. The expected error in estimation of ( $m - M$ ) by visual fitting of the theoretical models to the observations is of the order of 0.1 mag. The error on the age is mainly due to the visual fitting, which is ex-

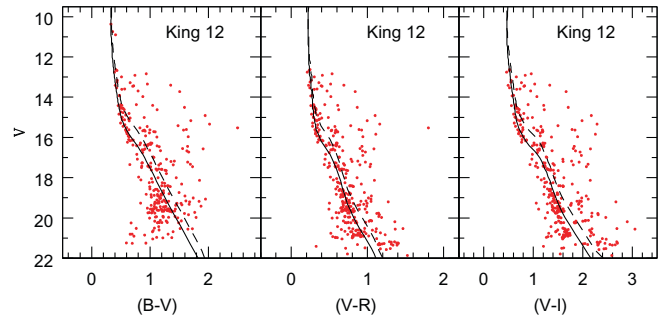


**Fig. 8.** The statically cleaned colour-magnitude diagram for King 12. Data of three brighter stars have been taken from Mohan and Pandey (1984). The solid line represents model by Girardi et al. (2002) and dashed line is the same model but for the binary stars.

pected to be  $\sim 0.1$  in the logarithmic scale of ages except for NGC 7226 (see Table 4).

The cluster Be 7 is one of the youngest clusters in the present sample. Phelps and Janes (1994) estimated its age as  $\sim 4$  Myr, whereas in the present work we estimated its age 12.58 Myr. The present estimation for reddening, distance modulus and age are in fair agreement with those given by Phelps and Janes (1994). The cluster NGC 2236 has well defined MS and significant number of evolved stars. We have determined the distance modulus and  $\log(\text{age})$  of the cluster as 14.0 mag and 8.7. This cluster is the oldest cluster in the present sample. The values of distance modulus and  $\log(\text{age})$  listed in WEBDA are 13.82 mag and 8.54 which match with the present observations. The present distance modulus and age for NGC 2236 also agree with those derived by Rahim (1970) and Babu (1991). The present derived  $\log(\text{age})$  for cluster the NGC 7226 is  $\log(\text{age}) = 8.4$  which is in agreement with the age listed in WEBDA ( $\log(\text{age}) = 8.4$ ) and the value ( $\log(\text{age}) = 8.6$ ) derived by Viskum et al. (1997), while present distance estimation is somewhat larger (about twice) than that given in the WEBDA. The age and distance of cluster King 12 given in Mohan and Pandey (1984) are based on *UBV* photoelectric data. However, the distance modulus ( $m - M$ ) = 14.1 mag obtained in the present study seems comparable with the distance modulus estimated by Mohan and Pandey (1984). The value of  $\log(\text{age})$  given by Mohan and Pandey (1984) matches well with the present value of  $\log(\text{age}) = 7.1$ .

## 5. Luminosity and mass function

The MS luminosity function (LF) is estimated by counting number of stars in magnitude bin. The star counts have been made in 1.0-mag bins in *V* of the stars lying inside the strip. The LF can be converted into mass function (MF) using the theoretical models. We used the model by Girardi et al. (2002) to convert the LF to MF. The MS LF for the core, corona and whole cluster region are derived using the statistically cleaned *V/V - I* CMDs and these are given in Table 5. The obtained MFs for the core, corona and whole cluster region are shown in Fig. 9.

The MF generally follows the power law,  $N(\log M) \propto M^\Gamma$ , and the slope of the MF is given as:

$$\Gamma = d \log N(\log M) / d \log M$$

where  $N(\log M)$  denotes the number of stars in a logarithmic mass bin and  $\Gamma$  is the MF slope. The classical value derived by Salpeter (1955) for the slope of IMF in the solar neighbourhood for the mass range  $0.4 < M/M_\odot < 10$  is  $\Gamma = -1.35$ . The values of the MF slopes in the core, corona and whole cluster region are given in Table 6. The slopes of the MF in the clusters Be 7, NGC 2236 and King 12 for whole cluster are found to be comparable with the Salpeter value,

**Table 4**

Reddening, age and distance of the clusters.

Cluster	$E(B - V)$ (mag)	Log (age)	$(m - M)$ (mag)	d (kpc)	$\text{Log (age)}_{lit}$	$(m - M)_{lit}$ (mag)	$d_{lit}$ (kpc)	$E(B - V)_{lit}$ (mag)
Cz 4	$0.55 \pm 0.05$	$7.6 \pm 0.1$	$14.1 \pm 0.1$	3.01	–	–	–	–
Be 7	$0.74 \pm 0.05$	$7.1 \pm 0.1$	$14.4 \pm 0.1$	2.64	6.60	14.53	2.57	0.80
NGC 2236	$0.56 \pm 0.05$	$8.7 \pm 0.1$	$14.0 \pm 0.1$	2.84	8.54	13.82	2.93	0.48
NGC 7226	$0.60 \pm 0.05$	$8.4 \pm 0.2$	$15.6 \pm 0.1$	5.60	8.45	13.75	2.62	0.54
King 12	$0.58 \pm 0.05$	$7.1 \pm 0.1$	$14.1 \pm 0.1$	2.89	7.04	13.71	2.38	0.59

**Table 5**Luminosity function of the target clusters.  $N$  is the number of probable cluster members in various magnitude bins.

Range in V mag	N														
	Cz 4			Be 7			NGC 2236			NGC 7226			King 12		
	Whole cluster	Core	Corona	Whole cluster	Core	Corona	Whole cluster	Core	Corona	Whole cluster	Core	Corona	Whole cluster	Core	Corona
11–12	2	2	–	1	–	1	–	–	–	–	–	–	–	–	–
12–13	7	2	5	4	1	4	1	–	1	–	–	–	4	3	1
13–14	7	3	4	–	–	–	2	2	0	–	–	–	8	5	3
14–15	18	6	12	7	2	6	19	2	17	12	2	10	14	5	9
15–16	14	–	14	16	2	10	27	4	23	26	7	19	24	2	22
16–17	17	4	13	16	–	15	35	5	30	35	2	33	24	3	21
17–18	27	4	23	22	–	20	43	4	39	38	6	32	22	2	20
18–19	11	3	8	28	2	26	70	12	58	49	2	47	29	1	28
19–20	13	–	13	18	1	16	43	6	37	65	2	63	49	3	46
20–21	1	–	1	4	–	4	24	3	21	18	10	17	10	2	8

whereas in the case of Cz 4 and NGC 7226 the value of slope is found to be shallower and steeper respectively, in comparison to the Salpeter value. However, the values of the slope of MF for all the clusters are comparable with  $3\sigma$  errors with the Salpeter value. Barring the case of NGC 2236 the value of  $\Gamma$  is found to be steeper in the outer regions of the clusters as compared to that of the core region. This suggests that a large number of low mass stars may have migrated towards the corona, indicating an effect of mass segregation.

**Table 6**MF slope  $\Gamma$  for core, corona and whole cluster region in the given mass range.

Cluster	Mass range $M_{\odot}$	$\Gamma$		
		Core	Corona	Whole cluster
Cz 4	0.83–7.55	$-0.43 \pm 0.20$	$-1.31 \pm 0.28$	$-0.88 \pm 0.19$
Be 7	0.89–10.99	$-0.61 \pm 0.09$	$-1.07 \pm 0.35$	$-1.19 \pm 0.26$
NGC 2236	0.87–2.93	$-0.93 \pm 0.32$	$-0.89 \pm 0.34$	$-1.14 \pm 0.52$
NGC 7226	0.90–3.73	$0.11 \pm 0.58$	$-2.16 \pm 0.15$	$-1.89 \pm 0.20$
King 12	0.88–13.30	$-0.28 \pm 0.20$	$-1.78 \pm 0.23$	$-1.28 \pm 0.18$

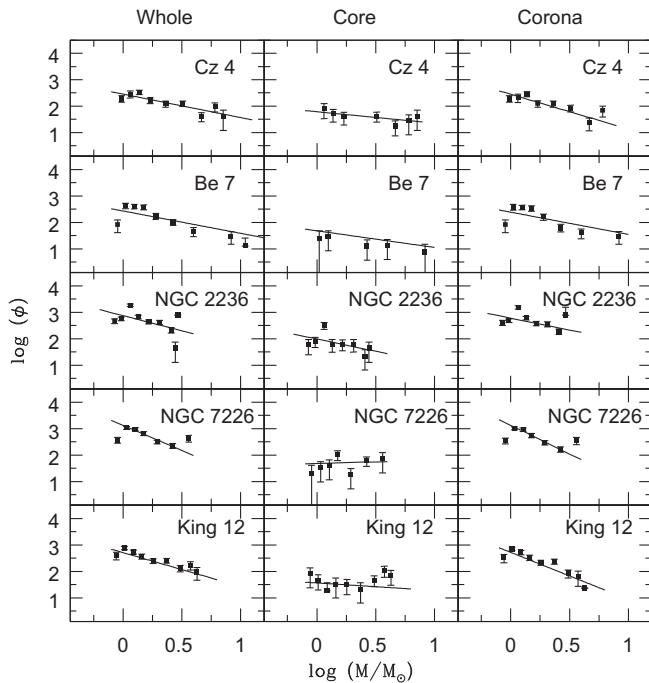


**Fig. 9.** The cluster mass functions for two sub-regions and whole cluster region.  $\text{Log}(\phi)$  represents  $\log(dN/d\log M)$ . The error bars represents  $\pm\sqrt{N}$  errors. Continuous lines show the a least squares fit to the data.

## 6. Dynamical evolution: mass segregation

The cumulative radial distribution for two mass groups is shown in Fig. 10. Effects of mass segregation are apparent in all the clusters under present study. The conclusion is further checked by using the Kolmogorov–Smirnov (KS) test. The confidence level ( $\geq 95\%$ ) confirms that the distribution of low mass stars are segregated from the massive ones, in the sense that massive stars are preferentially located towards the centre of the cluster.

To see whether the mass segregation present in the clusters is result of dynamical evolution, we have computed the dynamical evolution time,  $T_E$ , using the following relation

$$T_E = \frac{8.9 \times 10^5 \sqrt{N} R_h^{3/2}}{\sqrt{\bar{m}} \log(0.4N)}$$

where  $N$  is the number of cluster members,  $R_h$  is the radius within which half of the cluster mass is contained and  $\bar{m}$  is the average mass of the cluster stars (Spitzer and Hart, 1971). The value of  $R_h$ , assumed to be equal to half of the cluster extent, is given in Table 7. The total number of MS stars in the given mass range (see Table 6) are obtained with the help of the MF. A comparison of the cluster's age with their dynamical relaxation time  $T_E$ , given in Table 7, indicates that the former is larger than the latter. We conclude that all the clusters are dynamically relaxed and the observed mass segregation seems to have reached some level of dynamical relaxation.

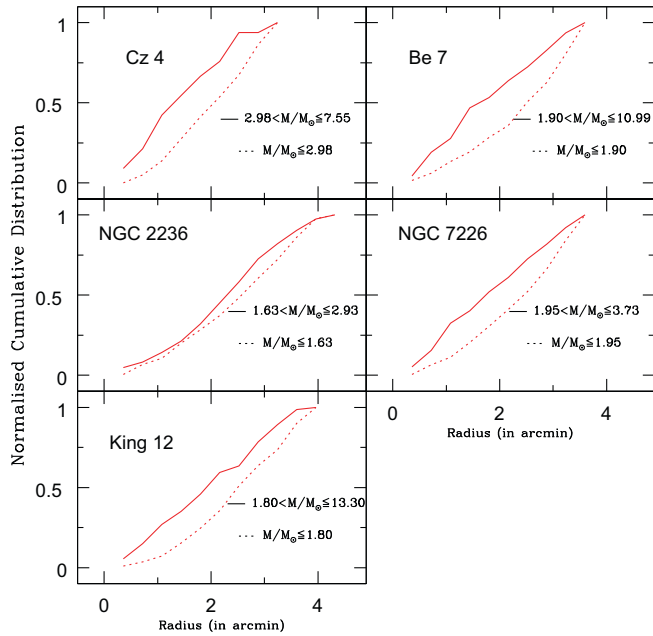


Fig. 10. The cumulative radial distribution of stars in different mass ranges.

Table 7

Various parameters for the target clusters in the given mass range (see Table 6) used for calculating the dynamical relaxation time  $T_E$ .

Cluster	N	$R_h$ (pc)	Mass ( $M_\odot$ )	$\bar{m}$ ( $M_\odot$ )	Age (Myrs)	$T_E$	$\tau$
Cz 4	117	1.46	$276 \pm 17$	2.35	39.8	6.6	5.97
Be 7	116	1.65	$235 \pm 14$	2.03	125	8.57	14.59
NGC 2236	264	1.96	$370 \pm 26$	1.40	501	16.57	30.24
NGC 7226	247	2.04	$386 \pm 19$	1.56	251	16.35	15.35
King 12	187	1.30	$316 \pm 15$	1.68	125	7.43	16.82

In order to study the effects of the dynamical evolution on the MFs, we calculated dynamical evolution parameter for each cluster  $\tau$ , which is defined as,  $\tau = \text{age}/T_E$ . Table 7 lists the estimated values of  $\tau$  for each cluster. In Fig. 11, we plot the  $\Gamma$  as a function of  $\tau$ . To increase the sample we added data from Sharma et al. (2008) and Lata et al. (2010). Although the scatter is large, Fig. 11(a) and (b) show that a systematic decreasing trend in  $\Gamma$  with  $\tau$  as suggested by Sharma et al. (2008), particularly in the outer region of the clusters. Bonatto and Bica (2005) have also found the same. However, contrary to the findings of Bonatto and Bica (2005) and Maciejewski and Niedzielski (2007), we did not find any relation of MF slope for core region with  $\tau$ , and the same is concluded by Sharma et al. (2008). The relation of MF slope with  $\tau$  can be represented by following relation;

$$\Gamma = \Gamma_0 + \exp(a/\tau),$$

with  $\Gamma_0 = -1.89 \pm 0.14$  and  $a = -9.15 \pm 5.41$  for the whole cluster region;  $\Gamma_0 = -2.07 \pm 0.13$  and  $a = -8.77 \pm 4.10$  for outer region. To study the effects of external interactions as well as internal gravitational interactions on the mass segregation, a quantity  $\Delta\Gamma = \Gamma_{\text{core}} - \Gamma_{\text{corona}}$ ; is plotted as a function of  $\log(\text{age})$ ,  $\tau$ , and  $R_G$  in Fig. 12. The Galactocentric distance,  $R_G$ , has been calculated assuming distance between Sun and Galactic centre as 8.5 kpc. Fig. 12(a) does not show any relation between  $\Delta\Gamma$  and  $\log(\text{age})$ . The  $\Delta\Gamma$  seems to decrease with  $\tau$  (Fig. 12(b)) as suggested by Sharma et al. (2008). The decrease in  $\Delta\Gamma$  with  $\tau$  can be interpreted as

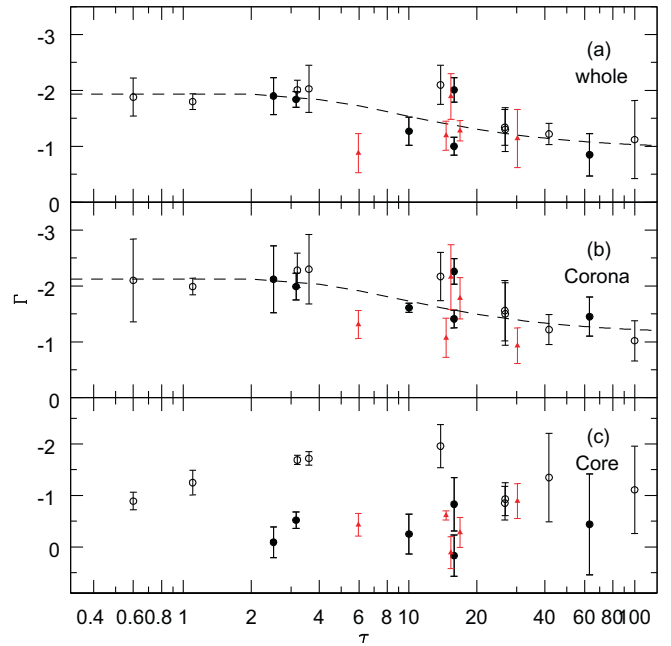


Fig. 11. Variation of  $\Gamma$  as a function of  $\tau$  ( $\text{age}/T_E$ ) for the whole cluster, corona and core regions of the clusters. Triangles, filled and open circles represent data from present study, Lata et al. (2010) and Sharma et al. (2008) respectively. The curve represents a function  $\Gamma = \Gamma_0 + \exp(a/\tau)$ .

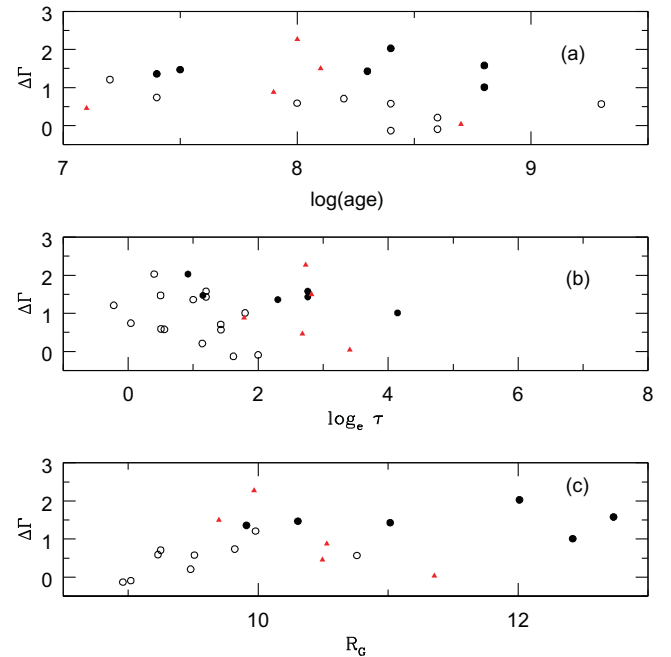


Fig. 12. Variation of  $\Delta\Gamma$  as function a of  $\log(\text{age})$ ,  $\tau$  and Galactocentric distance ( $R_G$ ). The symbols are same as in Fig. 11.

evaporation of low mass stars from the outer region. Fig. 12(c) also indicates a systematic variation of  $\Delta\Gamma$  as a function of Galactocentric distance except NGC 2236, indicating that evaporation of low mass members from outer region of the clusters is not significant at larger Galactocentric distances. Cluster NGC 2236 does not follow the trend due to fact that it is the oldest cluster in the present sample and located towards the Galactic centre. This scenario could be interpreted as the dynamical evolution drives the star cluster toward core collapse; the most massive stars segregate to the cluster



centre while lower mass stars segregate to the cluster halo. At the same time the cluster halo is stripped by the Galactic tidal field. The low mass stars therefore tend to be lost from the cluster at larger distances from the Galactic centre while higher mass stars can reach farther in *McMillan and Portegies Zwart (2001)*. Here we would like to point out that more sample is needed to get a conclusive view about variation of  $\Delta\Gamma$  with  $\log(\text{age})$ , dynamical evolution parameter ( $\tau$ ) and Galactocentric distance ( $R_G$ ).

## 7. Summary

This work presents *UBVRI* CCD photometry of five open clusters namely Cz 4, Be 7, NGC 2236, NGC 7226 and King 12. Fundamental parameters such as cluster extent, reddening  $E(B - V)$  and distance to the cluster have been obtained using the optical data. The cluster extents are 3.5 arcmin for Cz 4, 4.1 arcmin for Be 7, 4.4 arcmin for NGC 2236, 3.7 arcmin for NGC 7226 and 4.0 arcmin for King 12. The values of reddening  $E(B - V)$  for the Cz 4, Be 7, NGC 2236, NGC 7226 and King 12 are estimated as 0.55, 0.74, 0.56, 0.60 and 0.58 mag respectively. The ages of the clusters have been derived by visually fitting the theoretical models to the observed data points. The ages for present cluster sample range from  $\sim 10$  Myrs to  $\sim 500$  Myrs. The mass function slope for whole cluster region of the present cluster sample is found to be comparable to the Salpeter value. All the clusters show effects of mass segregation. The ages of the clusters are larger than their relaxation times, indicating that all the cluster are dynamically relaxed. The decrease in  $\Delta\Gamma (= \Gamma_{\text{core}} - \Gamma_{\text{corona}})$  with  $\tau (= \text{age}/T_E)$  can be interpreted as evaporation of low mass stars with time from the outer region of the cluster.

## References

- Andersen, J., Nordström, B., 2000. Stellar Clusters and Associations: Convection, Rotation, and Dynamos. In: Pallavicini, R., Micela, G., Sciortino, S., (Eds.), Proceedings from ASP Conference, vol. 198., p. 171. ISBN: 1-58381-025-0.
- Ann, H.B., Lee, S.H., 2002. JKAS 35, 29.
- Babu, G.S.D., 1991. JApA 12, 187.
- Bonatto, C., Bica, E., 2005. A&A 437, 483.
- Bonatto, C., Lima, E.F., Bica, E., 2012. A&A 540, 137.
- Carraro, G., 2006. BASI 34, 153.
- Carraro, G., Geisler, D., Moitinho, A., et al., 2005. A&A 442, 917.
- Chen, W.P., Chen, C.W., Shu, C.G., 2004. AJ 128, 2306.
- de la Fuente Marcos, R., 1997. A&A 322, 764.
- de la Fuente Marcos, R., 2002. Modes of Star Formation and the Origin of Field Populations. In: Eva, K., Grebel, Brandner, W., (Eds.), ASP Conference Proceedings, vol. 285., Astronomical Society of the Pacific, San Francisco. p. 174. ISBN: 1-58381-128-1.
- Girardi, L., Bertelli, G., Bressan, A., Chiosi, C., Groenewegen, M.A.T., Marigo, P., Salasnich, B., Weiss, A., 2002. A&A 391, 195.
- Kaluzny, J., Udalski, A., 1992. Acta Astron. 42, 29.
- Kang, Y.W., Ann, H.B., 2002. JKAS 35, 87.
- Landolt, A.U., 1992. AJ 104, 340.
- Lata, S., Pandey, A.K., Kumar, B., Bhatt, H., Pace, G., Sharma, G., 2010. AJ 139, 378.
- Maciejewski, G., 2009. Bulgarian Astron. J. 11, 67.
- Maciejewski, G., Niedzielski, A., 2007. A&A 467, 1065.
- Orekhova, L.K., Shashkina, L.P., 1987. Astronomical-geodetical investigations. Statistical Methods, pp. 4–14.
- McMillan, S.L.W., Portegies Zwart, S.F., 2001. AAS 199, 7906.
- Mohan, V., Pandey, A.K., 1984. Ap&SS 105, 315.
- Pandey, A.K., Mahra, H.S., 1986. Ap&SS 126, 167.
- Pandey, A.K., Bhatt, B.C., Mahra, H.S., 1988. A&A 189, 66.
- Pandey, A.K., Sharma, S., Upadhyay, K., Ogura, K., Sandhu, K., Mito, H., Sagar, R., 2007. PASJ 59, 457.
- Pataf, F., Carraro, G., 1995. A&ASS 114, 281.
- Phelps, R.L., Janes, K.A., 1994. ApJS 90, 31.
- Rahim, M., 1970. A&A 9, 221.
- Sagar, R., Richtler, T., 1991. A&A 250, 324.
- Salpeter, E.E., 1955. ApJ 121, 161.
- Sandhu, T.S., Pandey, A.K., Sagar, R., 2003. A&A 408, 515.
- Sharma, S., Pandey, A.K., Ogura, K., Mito, H., Tarusawa, K., Sagar, R., 2006. AJ 132, 1669.
- Sharma, S., Pandey, A.K., Ogura, K., Taori, A., Pandey, K., Sandhu, T.S., Sagar, R., 2008. AJ 135, 1934.
- Spitzer, L., Hart, M.H., 1971. ApJ 164, 399.
- Stetson, P.B., 1987. PASP 99, 191.
- Stetson, P.B., 1992. ADASS 1, 297.
- Tanikawa, A., Fukushige, T., 2005. PASJ 57, 155.
- Theuns, T., 1992. A&A 259, 493.
- Viskum, M., Hernandez, M.M., Belmonte, J.A., Frandsen, S., 1997. A&A 328, 158.
- Yilmaz, F., 1970. A&A 8, 213.